HOSTED BY

ELSEVIER

Available online at www.sciencedirect.com

ScienceDirect

The Crop Journal

Transcriptome analysis reveals key differentially expressed genes involved in wheat grain development

Yonglong Yu[a,1], Dong Zhu[a,1], Chaoying Ma[a,1], Hui Cao[a,1], Yaping Wang[a], Yanhao Xu[b], Wenying Zhang[b], Yueming Yan[a,b,*]

[a]College of Life Sciences, Capital Normal University, Beijing 100048, China
[b]Hubei Collaborative Innovation Center for Grain Industry/Yangtze University, Jingzhou 434025, China

ARTICLE INFO

Article history:
Received 18 December 2015
Received in revised form
8 January 2016
Accepted 2 February 2016
Available online 13 February 2016

Keywords:
Wheat
Transcriptome microarray
Differentially expressed genes
Grain development

ABSTRACT

Wheat seed development is an important physiological process of seed maturation and directly affects wheat yield and quality. In this study, we performed dynamic transcriptome microarray analysis of an elite Chinese bread wheat cultivar (Jimai 20) during grain development using the GeneChip Wheat Genome Array. Grain morphology and scanning electron microscope observations showed that the period of 11–15 days post-anthesis (DPA) was a key stage for the synthesis and accumulation of seed starch. Genome-wide transcriptional profiling and significance analysis of microarrays revealed that the period from 11 to 15 DPA was more important than the 15–20 DPA stage for the synthesis and accumulation of nutritive reserves. Series test of cluster analysis of differential genes revealed five statistically significant gene expression profiles. Gene ontology annotation and enrichment analysis gave further information about differentially expressed genes, and MapMan analysis revealed expression changes within functional groups during seed development. Metabolic pathway network analysis showed that major and minor metabolic pathways regulate one another to ensure regular seed development and nutritive reserve accumulation. We performed gene co-expression network analysis to identify genes that play vital roles in seed development and identified several key genes involved in important metabolic pathways. The transcriptional expression of eight key genes involved in starch and protein synthesis and stress defense was further validated by qRT-PCR. Our results provide new insight into the molecular mechanisms of wheat seed development and the determinants of yield and quality.

1. Introduction

Wheat (*Triticum aestivum* L., 2*n* = 6*x* = 42, AABBDD), an allohexaploid species, is the principal food crop used for humans and livestock globally. Wheat is counted among the "big three" cereal crops and is unrivaled in its range of cultivation owing to its extensive agronomic adaptability, high yield potential, and nutritional profile (including

* *Corresponding author*. Tel./fax: +86 10 68902777.
E-mail address: yanym@cnu.edu.cn
[1] These authors contributed equally to this work.
Peer review under responsibility of Crop Science Society of China and Institute of Crop Science, CAAS.

http://dx.doi.org/10.1016/j.cj.2016.01.006

essential amino acids, minerals, vitamins, beneficial phytochemicals, and dietary fiber) [1,2].

Cereal seeds consist of two main tissue fractions: starchy endosperm/aleurone and embryo/scutellum. The starchy endosperm of mature wheat seeds is a major source of nutrition, as well as the primary site for the storage of starch and proteins important for grain yield and flour quality [3,4]. The aleurone is a single cell thick and has two biological roles: (1) digesting the starchy endosperm to release nutrients and amino acids to the germinating embryo and (2) protecting the endosperm from stress and pathogens [5]. In addition, the wheat seed aleurone layer is the most concentrated source of vitamins and minerals and is also rich in proteins and lipids [6].

Starch and protein are the principal storage reserves in the wheat seed. Wheat seed development includes five main phases: fertilization (0 days post-anthesis [DPA]), "coenocytic" endosperm (1–5 DPA), cellularization, and early grain-filling (6–13 DPA), maximum grain filling (14–24 DPA), and desiccation (25–38 DPA). In general, the grain-filling period is considered to comprise cellularization and the early and maximum grain-filling phases [7].

Seed development is a very important stage in the cereal crop seed life cycle. The nutritive reserves of mature wheat seeds provide not only human food and livestock feed but also the energy for seed germination. Initial primary studies on seed development focused mainly on seed physiology and biochemistry [8], providing us with a basic understanding of the seed development process. In recent years, proteomics has been used to study the biochemical mechanisms of plant seed development, including barley [9], *Cunninghamia lanceolata* [10], *Medicago truncatula* [11,12], *Lotus japonicus* [13] and wheat [14]. However, the number of proteins identified by the proteomics approach is limited and does not permit a complete genome-wide comparison. Dry mature seeds of crops contain a vast number of mRNA species, which were first identified in cotton [15]. Since the 1990s, stored RNA in the mature dry seeds of plant species has been shown to be universal [16–18], and gene expression patterns can be detected in stored seed mRNA. Affymetrix arrays can provide a comprehensive, real-time picture of changes at the whole-transcriptome level during seed development, and this tool has been used to investigate the biological processes of wheat grain development [6,19,20]. Although transcriptome analysis during wheat grain development by RNA-Seq has been performed [21], studies of the comprehensive dynamic transcriptional characterization of grain filling stages are still limited.

Modern allohexaploid wheat has a huge and complex genome (up to 17,000 Mb) composed of the ancestral A, B, and D genomes. Recently, there has been much progress in wheat genome sequencing [22]. The A^u genome in *Triticum urartu* and D^t genome in *Aegilops tauschii* are the progenitors of the A and B genomes, respectively, of hexaploid wheat. Studies of the A^u and D^t genomes have recently been completed [23,24] and will facilitate further proteomics and transcriptomics research on wheat seed development. In the present study, we used an elite Chinese bread wheat cultivar (Jimai 20) with high yield, wide adaptability, and superior quality [25] to perform a dynamic transcriptome microarray analysis during grain-filling stages using the GeneChip Wheat Genome Array (Affymetrix, Santa Clara, CA, USA). We identified key differentially expressed genes involved in grain development. Our results shed new light on the molecular mechanisms of the accumulation of nutritive reserves in wheat, as well as the determinants of yield and quality.

2. Materials and methods

2.1. Plant material and field experiment

The wheat cultivar Jimai 20 was planted at the experimental station of Chinese Agricultural University, Beijing, in the 2013 to 2014 growing season. Experiments were performed in three biological replicates (each plot with 50 m^2). Cultivation and management followed local field production conditions. Grain samples were harvested at 11, 15, and 20 days post-anthesis (DPA). The collected samples were immediately placed in liquid nitrogen and stored at −80 °C until use.

2.2. Grain ultrastructure observation by scanning electron microscope (SEM)

Grain samples harvested at 11, 15, and 20 DPA were placed in fixative (5 mL 38% formalin, 5 mL glacial acetic, 90 mL 70% ethyl alcohol) for more than 12 h. Sequentially, the samples were dehydrated in 70% ethanol solution (20 min), 80% ethanol solution (20 min), 90% ethanol solution (overnight), and 100% ethanol solution (20 min). The samples were then treated stepwise for 20 min each in mixtures of ethanol and isoamyl acetate with ratios 3:1, 1:1, and 1:3 before soaking in isoamyl acetate. Finally, critical-point drying was performed for SEM observation. Observation of grain endosperm ultrastructures was performed with a SEM S-4800 FESEM instrument (Hitachi, Japan).

2.3. RNA isolation, microarray hybridization, and data treatments

Total RNAs isolation and microarray hybridization were performed as described previously [2]. All microarray data from the three biological replicates obtained in this study were deposited in the NCBI GEO database and are accessible under GEO Series accession number GSE75561 (http://www.ncbi.nlm.nih.gov/geo/query/acc. cgi?acc=GSE75561).

2.4. Filter of multi-class differential genes

As the random variance model (RVM) *F*-test can raise degrees of freedom effectively in the cases of small samples, it was applied to filter the differentially expressed genes for the control and experiment group. The differentially expressed genes were selected based on *P*-value threshold after significance analysis and false discovery rate (FDR) analysis [26–28].

2.5. Series test of cluster (STC) and gene ontology (GO) annotation analysis of differential genes

According to the random variance model (RVM) corrective ANOVA, the series test of cluster (STC) was performed by selecting differential expression genes. In accordance with the

different signal density change tendency of genes under different situations, we identified a set of unique model expression tendencies. The raw expression values were converted into $\log_2$ ratios. Some unique profiles were further defined using a strategy for clustering short time-series gene expression data. The expression model profiles are involved in the actual or the expected number of genes assigned to each model profile. Fisher's exact test and multiple-comparison tests were used to determine whether the significant profiles had higher probability than expected [29,30]. Gene ontology (GO) analysis of genes showing certain specific tendencies was performed following Dong et al. [31] to identify the main functions of genes with the same expression trend [32,33].

2.6. MapMan analysis

In the MapMan analysis [2], input files were created by calculating the natural log ratio of the three control samples to the mean detection in the treatment samples. Genes were considered as not expressed under the respective experimental condition if they were absent in two of the three replicates. Final analyses were performed with MapMan version 1.6.1 [34], including the automatic application of the Wilcoxon rank sum test. Entire data sets from NascArrays and from Nakabayashi et al. [35] were downloaded to allow comparison with public Affymetrix ATH1 data sets.

2.7. Metabolic pathway analysis

To identify significant pathways of differentially expressed genes, pathway network analysis was conducted using KEGG, Biocarta, and Reatome [2]. First, significant pathways were selected using Fisher's exact test and χ^2 test, in which *P*-value (<0.05) and FDR (<0.05) were used to define the threshold of significance. The enrichment Re was calculated according to previous reports [36–38]. The Path–Net, the interaction net of the significant pathways of the differentially expressed genes, was constructed through the interaction among pathways of the KEGG database, which was used to directly and systemically identify interactions between significant pathways. The Path–Net summarizes the pathway interaction of genes differentially expressed during disease and explains why certain pathways were activated [37].

2.8. Dynamic gene net analysis

Gene dynamic co-expression networks were built based on functional gene associations to identify gene interactions in biological processes, in which a net was constructed from significantly correlated gene pairs according to the calculation of the Pearson correlation for each pair [39]. In the net, cycle nodes and edges between the two nodes represent genes and interactions between genes, respectively. The network analysis was performed to locate the core regulatory factors (genes) showing the highest k-core values or degree values and showing connection with most adjacent genes. A k-core of the network represents a subnetwork in which all nodes are connected to at least *k* other genes. As a consequence, the rank of the k-core value shows the complexity of the gene association relationships, with the maximum core order in the graph considered the primary or highest k-core [40]. Cycles with identical colors are parts of the same subgraph [41,42]. We further analyzed the various properties of networks, in which the degree centrality, an important measure of gene centrality within a network, was constructed to estimate the relative importance.

2.9. Total mRNA extraction and qRT-PCR analysis

Total mRNA was extracted using TRIzol Reagent (Invitrogen) based on the manufacturer's instructions. A PrimeScriptRT reagent Kit with gDNA Eraser (TaKaRa) was used to remove genomic DNA and to synthesize the cDNA. Gene-specific primers were designed with the online tool Primer3Plus (http://www.bioinformatics.nl/cgi-bin/primer3plus/primer3plus.cgi). The primers were further checked by blasting primer sequences against the NCBI database (http://www.ncbi.nlm.nih.gov/tools/primer-blast/index.cgi?LINK_LOC=BlastHome). *ADP-ribosylation factor* (*ADP*) was selected as the reference gene. Transcription levels of genes were quantified with a CFX96 Real-Time PCR Detection System (Bio-Rad) based on the 2(−Delta Delta C(T)) method [43]. The intercalating dye SYBR Green was used, and the experiment was performed in a 20 μL volume reaction system containing 10 μL 2× SYBR Premix ExTaq (TaKaRa), 2 μL 10-fold diluted cDNA, 0.15 μL of each gene-specific primer, and 7.7 μL ddH_2O. The PCR running protocol was as follows: 95 °C for 3 min, 40 cycles at 95 °C for 20 s, 60 °C for 15 s, and 72 °C for 20 s. Three biological replicates and triplicates for each PCR reaction were performed for each gene. The qRT-PCR efficiency was detected by five serial 10-fold dilutions of cDNA. In addition, the PCR amplification efficiency (E) of 95–105% and correlation coefficient (R^2) of 0.994–1.000 were controlled.

3. Results

3.1. Grain morphology and ultrastructure changes during seed development

The accumulation of nutritive reserves (such as starch, sucrose, storage proteins, and lipids) begins in early grain development and continues until the seed matures. We harvested grain samples based on thermal times (the cumulative average daily temperature after anthesis, °C) corresponding to DPA: 252 °C (11 DPA), 353 °C (15 DPA), and 461 °C (20 DPA) in order to analyze gene expression patterns during grain development. In general, grain size and weight gradually increased from flowering to maturity. Morphology and SEM analysis showed that seed size gradually increased during grain development (Fig. 1-A), as did weight and accumulation of starch granules (Fig. 1-B and C). Wheat endosperm contains three kinds of starch granule: A-type (diameter > 10 μm), B-type (diameter 5–10 μm), and C-type (diameter < 5 μm), which accumulate during grain development and supply energy for seed germination. Previous observations have indicated that A-type starch granules appear at 6 DPA, while the B-type appears at 11 DPA [44,45]. Our results showed that A-type granule size and grain weight increased more rapidly from 11 to 15 DPA than during the subsequent phases, showing that the period 11–15 DPA is a

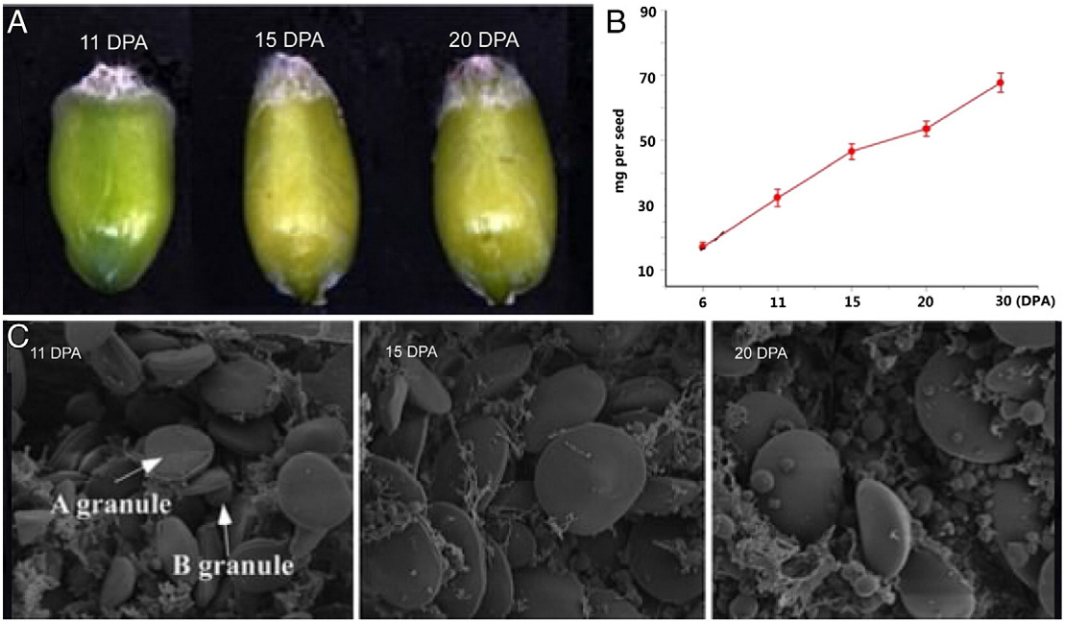

Fig. 1 – Grain morphological and ultrastructural changes during seed development. A. Changes in grain morphology. B. Changes in grain weight during the development process. C. Ultrastructural changes in wheat endosperm based on SEM observation. A- and B-granules are indicated.

key stage for the synthesis and accumulation of seed starch (Fig. 1-C).

3.2. *Transcriptome expression profiles and differential expression gene analysis during seed development*

Using transcriptome expression analysis using GeneChip Wheat Genome Arrays, we identified a total of 61,703 probe sets (the sum of 61,115 actual probe sets and the other 588 repeated probe sets), which could be classified into 35 bins representing 51,411 transcripts (Table S1, Table S2). Of these, 19,782 probe sets with different functions were classified with automatic annotations of metabolic pathways and large enzyme families. The other 41,921 probe sets were classified as "unknown" or "not assigned."

Genome-wide transcriptional profiling showed that extensive gene expression occurred during grain development. In total, 1904 differentially expressed probe sets corresponding to 1736 transcripts were discovered during three seed development phases (Table S3). To compare the numbers of up- or downregulated differential genes between two successive time points, we used significance analysis of microarrays (SAM) with a stringent 5% FDR (Table S4, Table S5). SAM plotsheet analysis (Fig. 2) showed that 8656 significantly differentially expressed genes were detected in the comparison of 11 to 15 DPA, of which 3105 genes were upregulated and the remainder downregulated. However, between 15 and 20 DPA, there were only 2101 significant differentially expressed genes, of which 1316 were upregulated and 785 downregulated. Apparently, there were 4-fold more differentially expressed genes between 11 and 15 DPA than between 15 and 20 DPA, suggesting that the former period is more important during reserve synthesis and accumulation.

3.3. *STC and GO annotation analysis of differentially expressed genes*

STC analysis of differentially expressed genes revealed 16 gene expression profiles that can be classified into four groups (Fig. 3). Among these 16 expression profiles, we identified 5 significant profiles, all belonging to groups I and II, based on their P values (Fig. S1, Fig. 3). As shown in Table S6, the upregulated genes in group I and downregulated genes in group II accounted for 67.6% of the total differentially expressed genes. The genes assigned to group III showed increased expression in the period 11–15 DPA, but were sharply downregulated in the next period. The genes assigned to group IV were downregulated between 11 and 15 DPA and upregulated after 15 DPA (Fig. 3). Among the five significant expression profiles, two major significant patterns (profile 2 in group I and profile 7 in group II) had the largest numbers of differentially expressed genes (294 and 169, respectively) (Fig. S1, Table S6).

To obtain an overview of differentially expressed genes involved in the five statistically significant differential expression patterns during seed development, we performed GO annotation and enrichment analysis. The GO annotation results are listed in Table S7. The distribution bar charts of the five profiles (profiles 2, 1, and 11 belonging to upregulated group I and profiles 7 and 4 belonging to downregulated group II) are shown in Fig. 4 according to the *P*-values of their annotations ($P < 0.05$). In profile 2, "response to water" (GO: 0009415, $P = 3.23E\text{-}10$) was the most significantly enriched term. "Chitin catabolic process" (GO: 0006032, $P = 3.72E\text{-}05$) and "cell wall macromolecule catabolic process" (GO: 0016998, $P = 0.000124$) were also significantly enriched (Fig. 4-A). In profile 1, "dicarboxylic acid transport" (GO: 0006835, $P = 0.000426$), "proteolysis" (GO: 0006508, $P = 0.000699$), and "response to oxidative stress" (GO: 0006979, $P = 0.008485$) were the top three

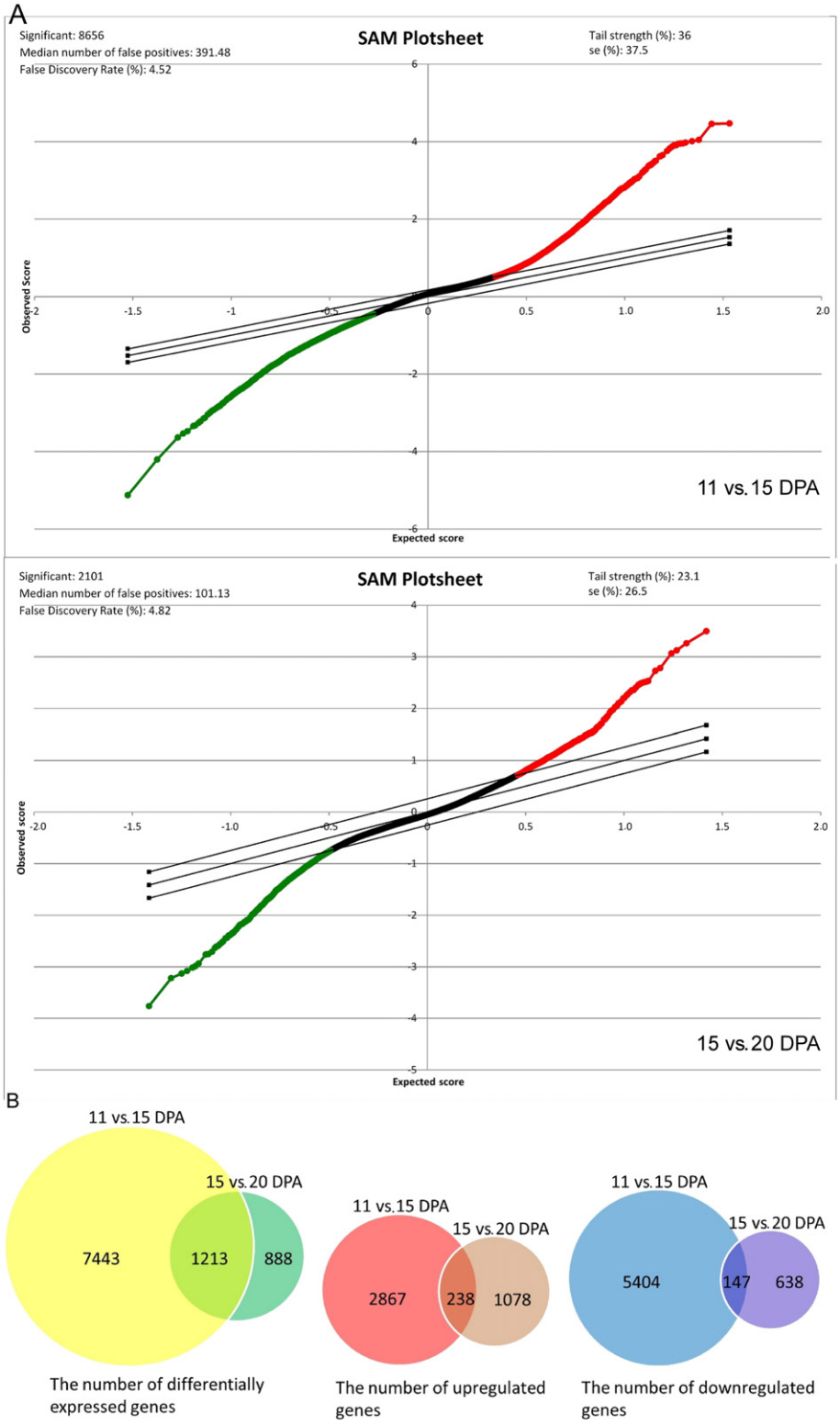

Fig. 2 – The number of differentially expressed genes. A. SAM Plot analysis displays significant difference genes in the periods 11–15 DPA and 15–20 DPA. B. Venn diagram analysis of the differentially expressed genes.

significantly overrepresented terms (Fig. 4-B). In profile 11, the top two significantly enriched terms were "chitin catabolic process" (GO: 0,006,032, $P = 0.000217$) and "cell wall macromolecule catabolic process" (GO: 0016998, $P = 0.000534$). "Positive regulation of cell division" (GO: 0051781, $P = 0.009934$) and "cell wall modification" (GO: 0042545, $P = 0.011779$) were also significant (Fig. 4-C). In profile 7, "metabolic process" (GO: 0008152, $P = 5.90E-05$) and "polysaccharide catabolic process" (GO:

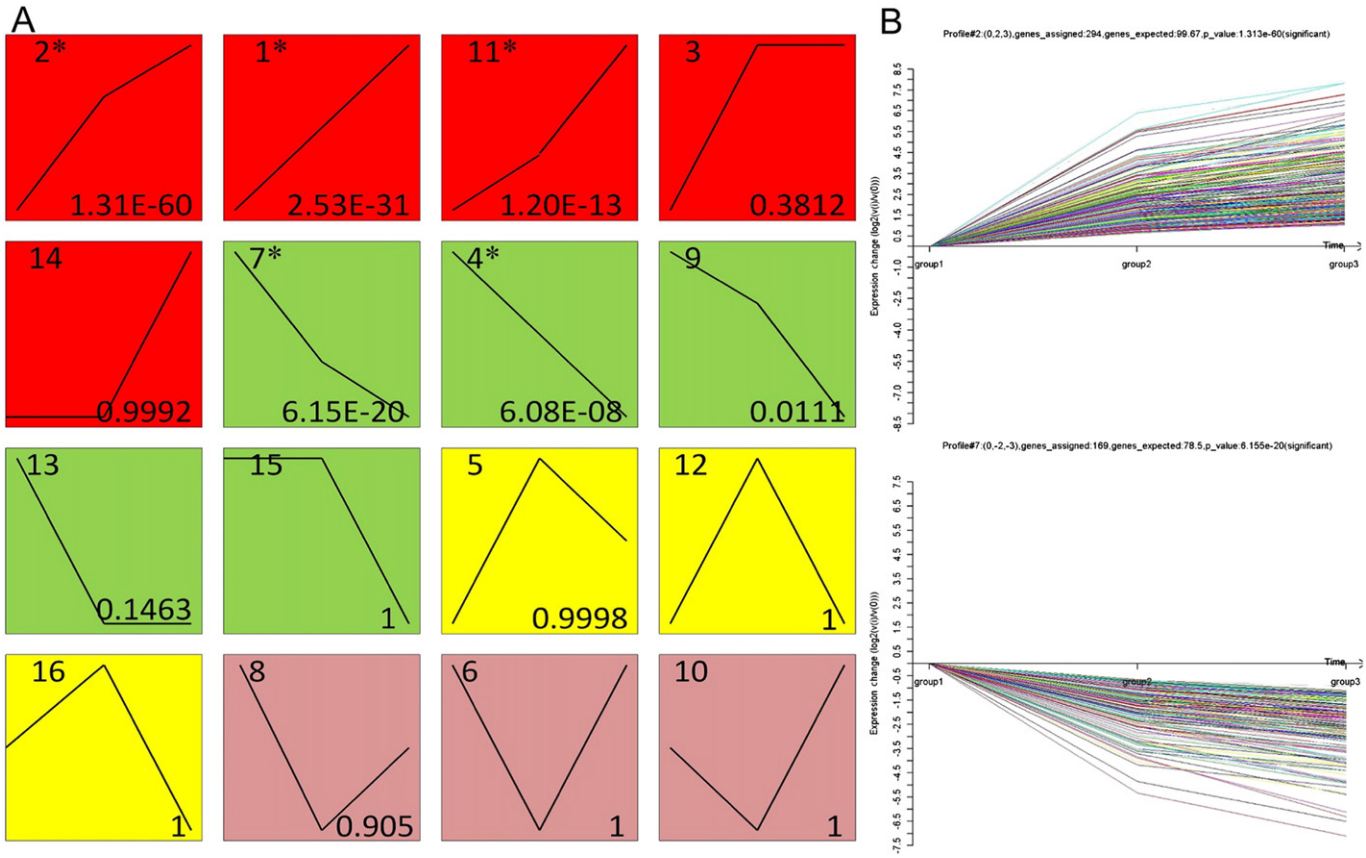

Fig. 3 – Gene expression patterns analyzed by model profile and two significant patterns (profiles 2 and 7). A. Each box represents a model expression profile. The upper number in the profile box is the model profile number and the lower number is the *P* value used to summarize the different gene expression patterns. In total, five expression patterns of genes showed significant *P*-values ($P < 0.05$) and are labeled with asterisk. The same color represents the same group. The model profiles marked with red (group I) represent upregulated expression patterns, whereas the green profile boxes (group II) represent downregulated expression patterns. Profiles 5, 12, and 16 (group III) belong to the pattern of genes that were upregulated first and then downregulated, whereas the remaining profile boxes (group IV) belong to the opposite pattern to that of group III. B. Profile 2 increased in expression and profile 7 decreased in expression during seed germination. The horizontal axis represents development phase and the vertical axis the time series of gene expression levels after log_2-normalized transformation.

0000272, $P = 0.006663$) were the top two terms (Fig. 4-D). In profile 4, "response to oxidative stress" (GO: 0006979, $P = 0.004654$), "oxidation reduction" (GO: 0055114, $P = 0.005996$), "lignin biosynthetic process" (GO: 0009809, $P = 0.011846$), and "peptidoglycan biosynthetic process" (GO: 0009252, $P = 0.017743$) were the top four significantly enriched terms (Fig. 4-E).

"Response to water" (GO: 0009415, $P = 3.23E-10$) and "metabolic process" (GO: 0008152, $P = 5.90E-05$) in profiles 2 and 7, respectively, were the two most significantly enriched terms. This suggests that genes related to water stress are upregulated and genes involved in metabolic process are downregulated during the period of grain-filling before desiccation (Fig. 4-A and D). Functional annotations associated with stress response and cell wall metabolism were detected frequently among the five profiles, suggesting that both functional groups are important during seed development.

We also performed GO analysis for all the differentially expressed genes, as listed in Table S7 and shown in Fig. 4-F ($P < 0.05$). We found that "proteolysis" (GO: 0006508, $P = 3.20E-08$), "response to water" (GO: 0009415, $P = 1.88E-05$), "chitin catabolic process" (GO: 0006032, $P = 2.45E-06$), "chromatin assembly or disassembly" (GO: 0006333, $P = 1.55E-05$), and "cell wall macromolecule catabolic process" (GO: 0016998, $P = 2.01E-05$) were most significantly overrepresented.

3.4. *Reserve accumulation and abiotic stress responses during seed development as revealed by MapMan analysis*

We used MapMan analysis to map transcriptome data, define functional categories, and identify significantly overrepresented functional groups, as well as to display important functional groups of genes activated in different stages of grain development (Fig. 5, Table S1, Table S2). Reserve accumulation in the endosperm, which can provide energy for seed germination, post-germination and growth, is initiated in early grain development and ends when the seed matures. The seed development stages (11–20 DPA) in this study involved mainly grain filling (reserve accumulation), which corresponds to the early grain-filling and maximum grain-filling stages [7].

Energy provision via the activation of glycolysis, the tricarboxylic acid (TCA) cycle, and mitochondrial electron

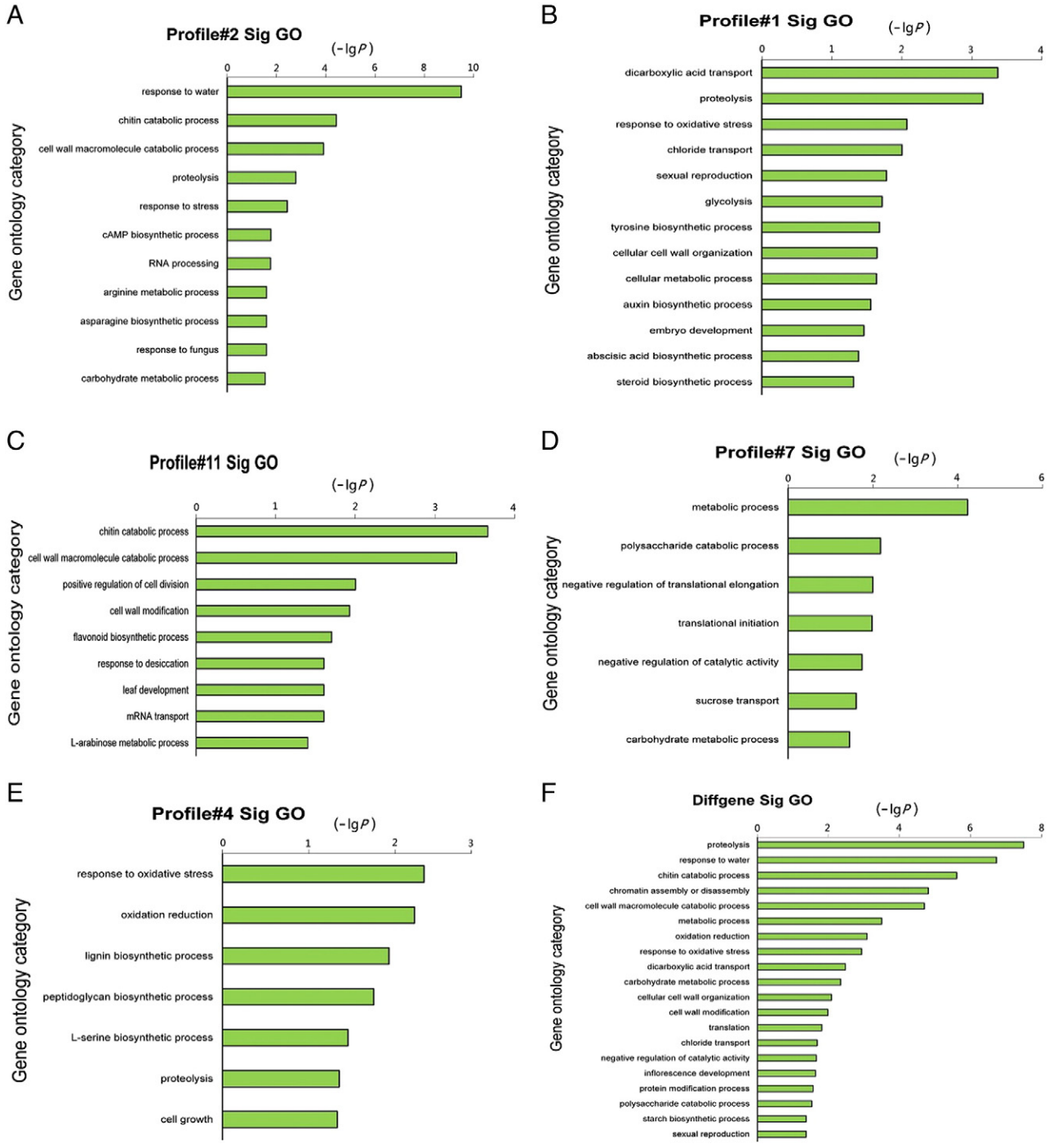

Fig. 4 – GO annotation analysis of five significant expression profiles and all the differentially expressed genes. A, B, C, D, and E show the GO analyses of five significant expression profiles, whereas the last, F, is the GO analysis of all the differentially expressed genes. Horizontal axis is –lg *P* (*P* is the abbreviate of *P*-value), vertical axis represents the different functional groups.

Fig. 5 – MapMan metabolism overview maps showing differences in transcript levels (11 vs. 15 and 15 vs. 20 DPA) during seed development. A. 11 vs. 15 HAI. B. 15 vs. 20 DPA. $\log_2$ ratios for average transcript abundance were based on three replicates of Affymetrix GeneChip Wheat Genome Array. The resulting file was loaded into the MapMan Image Annotator module to generate the metabolism overview map. On the logarithmic color scale, blue represents downregulated transcripts and red represents upregulated transcripts.

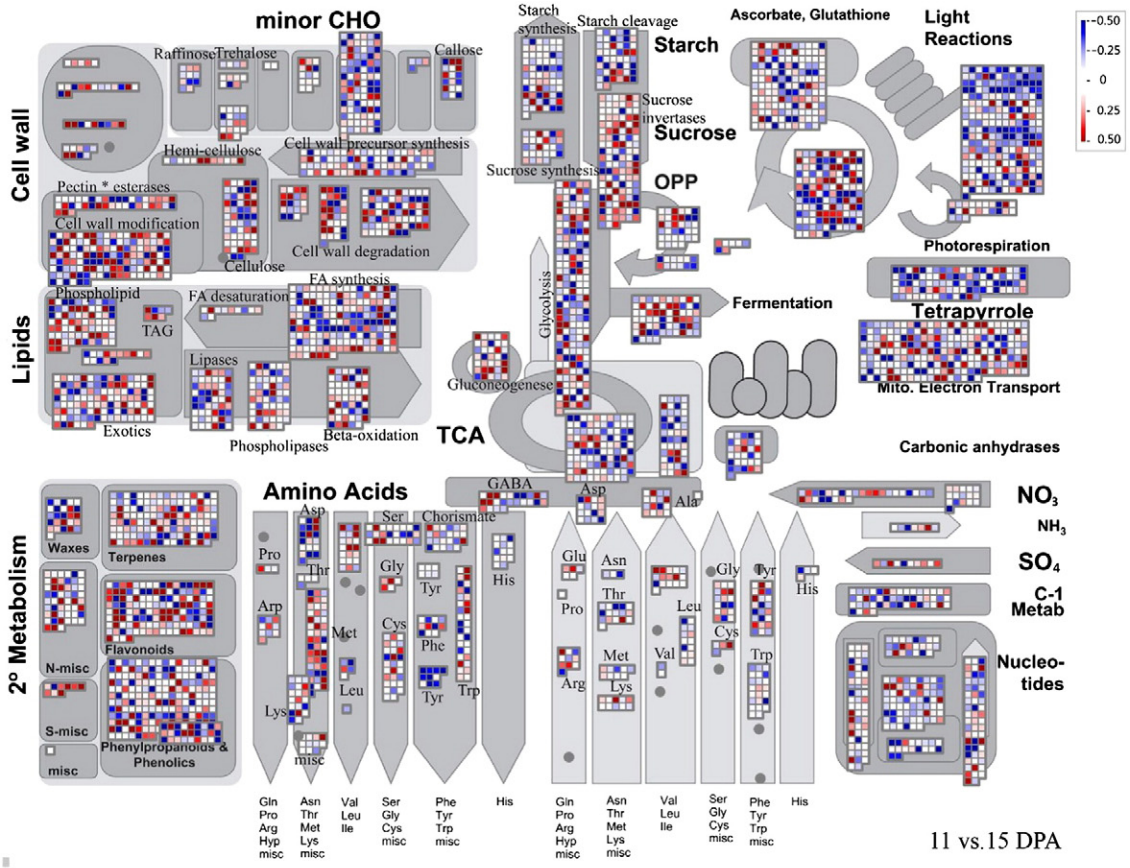

11 vs.15 DPA

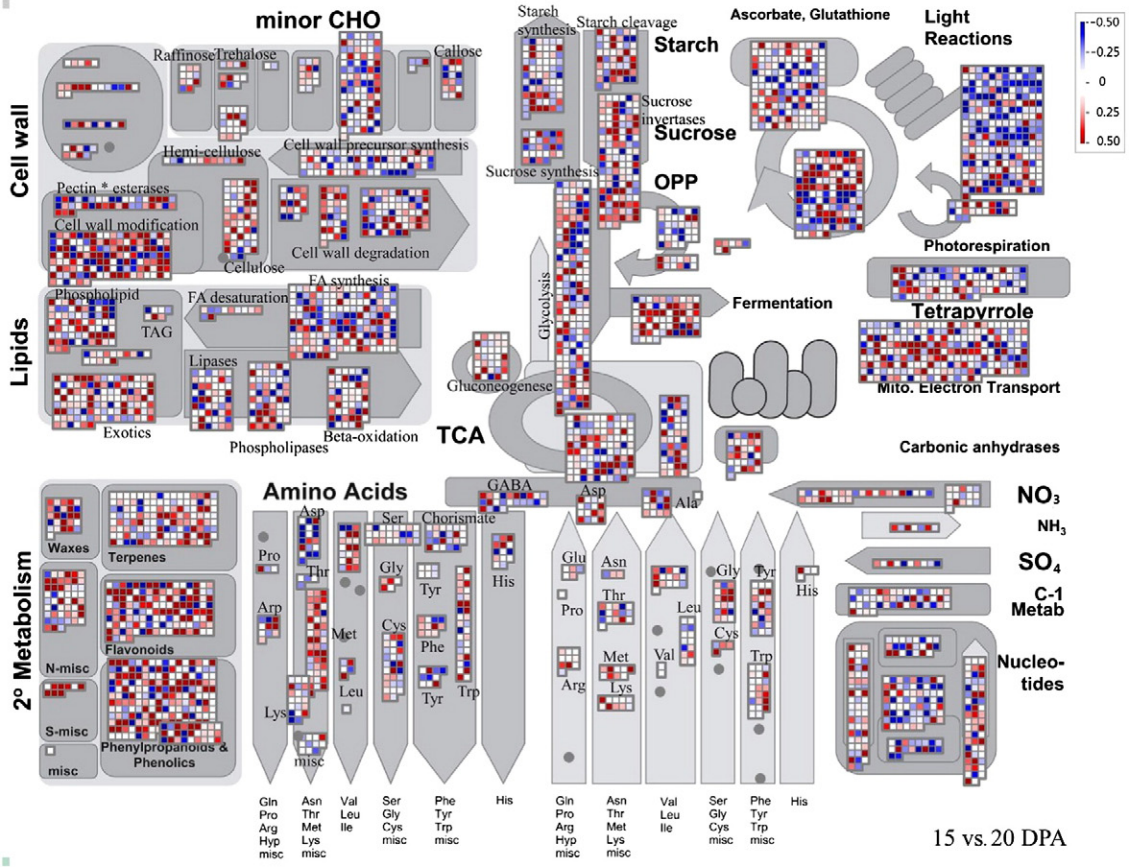

15 vs. 20 DPA

transportation are essential for grain development [14,46]. In our gene expression data, most genes involved in sucrose hydrolysis and glycolysis were upregulated, especially from 15 to 20 DPA (Fig. 5). Key enzymes involved in sucrose hydrolysis and glycolysis include sucrose invertase, hexokinase, phosphofructokinase (PPFK), and pyruvate kinase (PK). From 11 to 20 DPA, the expression values of genes CD454795 (encoding sucrose invertase) and BQ162543 (encoding hexokinase) increased 8-fold and 3-fold, respectively. The genes CA661266 (related to PPFK) and CA640211 (involved in PK) were strongly activated, while CA661266 and CA640211 showed distinct upregulation at 11–15 DPA and 15–20 DPA, respectively.

A large number of genes involved in starch synthesis were detected in our results. Starch synthesis genes are gradually activated and upregulated from 11 to 20 DPA, and sucrose synthesis-related genes followed a similar expression pattern (Fig. 5). As one of the key enzymes in the process of starch synthesis, sucrose synthase (SUSY) breaks down sucrose into fructose and glucose that are then converted into uridine diphosphate (UDPG) with catalysis by UDPG pyrophosphorylase (UGPase). UDPG is the glucose donor in the synthesis process for glycosides, oligosaccharides, polysaccharides, and related molecules. We found that the genes encoding SUSY (BJ277098 and CD453631) and UGPase (CA617830) had significantly upregulated expression during grain development. Previous studies have suggested that UGPase also couples with ADPG pyrophosphorylase (AGPase), another key rate-limiting enzyme in starch synthesis, to produce ADPG for starch synthesis [47,48]. In our data, we found an important gene (CA619571) related to AGPase that was upregulated from 11 to 20 DPA. The upregulation of these related genes contributes to the gradual accumulation of starch.

Protein synthesis depends on amino acid synthesis and accumulation. We found that genes related to the synthesis of common amino acids were activated from 11 to 15 DPA, and their expression levels increased significantly from 15 to 20 DPA (Fig. 5). In particular, the genes for methionine (Met) and aspartic acid (Asp) synthesis, two important amino acids for protein synthesis, were strongly upregulated, indicating an acceleration in protein synthesis during the 15–20 DPA period.

The MapMan cellular response overview visualization tool revealed cell stress responses during seed development (Fig. 6). The majority of heat transcripts associated with abiotic stress were upregulated from 11 to 15 DPA, and their expression continued to increase until 20 DPA. The upregulation of cold, drought/salt, and touch/wounding transcripts was more pronounced at 15–20 DPA than at 11–15 DPA. Heme serves as a key enzyme for clearing H_2O_2 in antioxidant pathways and was active mainly from 11 to 15 DPA. After 15 DPA, the genes associated with heme were downregulated (Fig. 6).

3.5. *Metabolic pathway network analysis*

We established a network for metabolic pathways (Fig. 7). According to the degree value (Table S8), glycolysis/gluconeogenesis, pyruvate metabolism, and the TCA cycle were the top three metabolic pathways. Starch synthesis during grain-filling was the top contributor to nutritive reserve accumulation, followed by protein synthesis. One important pathway is starch and sucrose metabolism (colored orange in Fig. 7). The source and target pathways for starch and sucrose metabolism both suggest that glycolysis/gluconeogenesis and pentose and glucuronate interconversion play direct roles in starch and sucrose metabolism. Other pathways (such as the pentose phosphate pathway, pyruvate metabolism, and the TCA cycle) may play indirect roles in starch and sucrose metabolism. The pathways directly associated with protein synthesis include glycine, serine, and threonine metabolism (Gly, Ser, and Thr), which involve the main enzymes of protein metabolism (cysteine protease, serine protease, and threonine protease). The other essential amino acids are likely to participate indirectly in protein synthesis and degradation by affecting the metabolism of glycine, serine, and threonine. According to our results, lysine (Lys) and valine (Val) biosynthesis, as well as leucine and isoleucine (Leu and Ile) biosynthesis, are the source, as well the targets, of glycine, serine, and threonine metabolism (Gly, Ser, and Thr); thus, these amino acids play key roles in protein metabolism. Tyrosine (Tyr), phenylalanine (Phe), and arginine and proline (Arg and Pro) metabolism affect the pathways of Gly, Ser, and Thr metabolism through their roles in the TCA cycle, pyruvate metabolism, and glyoxylate and dicarboxylate metabolism. All of the major and minor metabolic pathways regulate one another to ensure regular seed development and nutritive reserve accumulation.

3.6. *Gene co-expression network with k-core algorithm*

To identify functional genes that play vital roles in wheat seed development, we created a gene coexpression network with a k-core algorithm using the genes involved in important metabolic pathways (Fig. 8). The most central genes have the highest degree values within the network. The interactions and their degrees, as well as k-core values, are listed in Table S9. Most genes were involved in stress response, major CHO metabolism, protein metabolism, hormone metabolism, cell wall metabolism, lipid metabolism, DNA/RNA processing, signaling, or development. Four of the most important core genes were located at key positions in the network BQ172037, encoding the thaumatin family and involved in abiotic stress (k-cores of 8 and 29 degrees); BJ294280, encoding TBC (Tre2/Bub2/Cdc16) and involved in the secretory pathway (k-cores of 9 and 28 degrees); CD490538, encoding an ara54-like RING finger protein and involved in abscisic acid metabolism (k-cores of 9 and 28 degrees); and CA717577, associated with biotic stress (k-cores of 8 and 28 degrees). These four genes directly regulated 112 neighboring genes (Table S9). BQ172037 was downregulated, whereas the other three genes were upregulated (Table S1, Table S2). BQ172037 and BJ294280 expressions were negatively correlated, suggesting that down/upregulation of abiotic stress genes leads to up/downregulation of secretory pathway genes and vice versa.

Protein metabolism, stress response, and major CHO metabolism during wheat seed development are important metabolic pathways. Our results show that BJ294280 (related to the secretory pathway and located at the center of the network) is a pivotal gene. According to the k-cores of BJ294280, 28 neighboring genes involved in stress response, cell wall, major CHO metabolism, development, RNA transcription regulation and hormone metabolism were regulated by BJ294280. Some of these regulated genes were downregulated, such as genes associated with abiotic stress, cell walls,

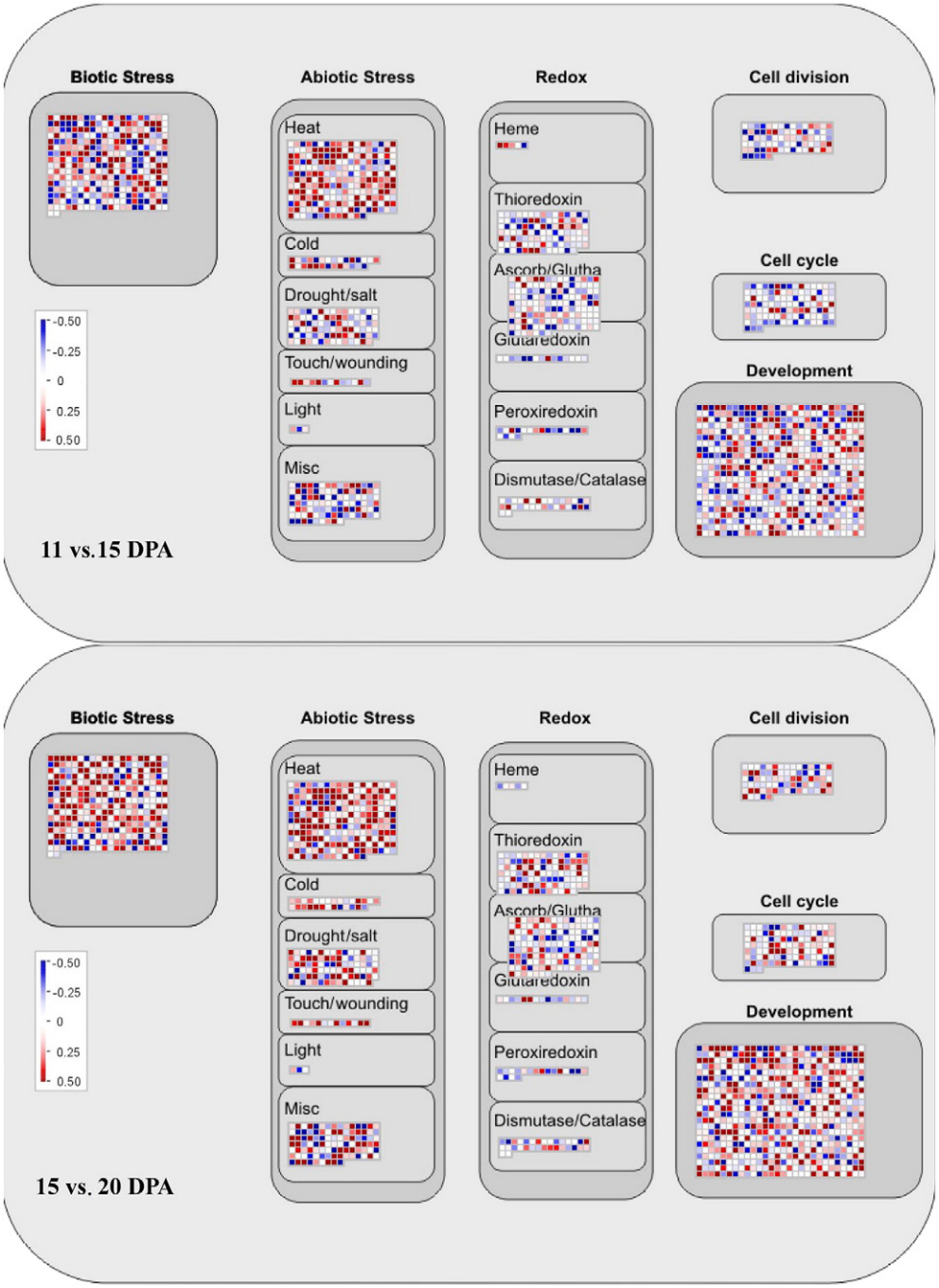

Fig. 6 – MapMan metabolic overview maps showing differences in transcript levels (11 versus 15 and 15 versus 20 DPA) of cellular response during seed development. For further details, see legend to Fig. 5.

and major CHO metabolism, whereas other genes were upregulated by BJ294280. The k-cores of all 28 co-expressed genes were greater than 6 (Table S9), indicating that these genes play key roles in seed development.

3.7. *Validation of key differentially expressed genes by qRT-PCR*

To validate the microarray data, the transcriptional expressions of eight key differentially expressed genes involved in starch and protein synthesis and stress defense were further analyzed by qRT-PCR (Fig. 9). The gene-specific primers used in this study are listed in Table S10 and the double standard curves and melting temperature curves as optimal performance parameters are shown in Fig. S4. The expression trends of the eight genes by qRT-PCR were highly consistent with those from cDNA microarray analysis (Table S1).

4. Discussion

The economic and nutritional importance of wheat grain depends on the accumulation of nutritive reserves during wheat seed development. Reserves include principally starch

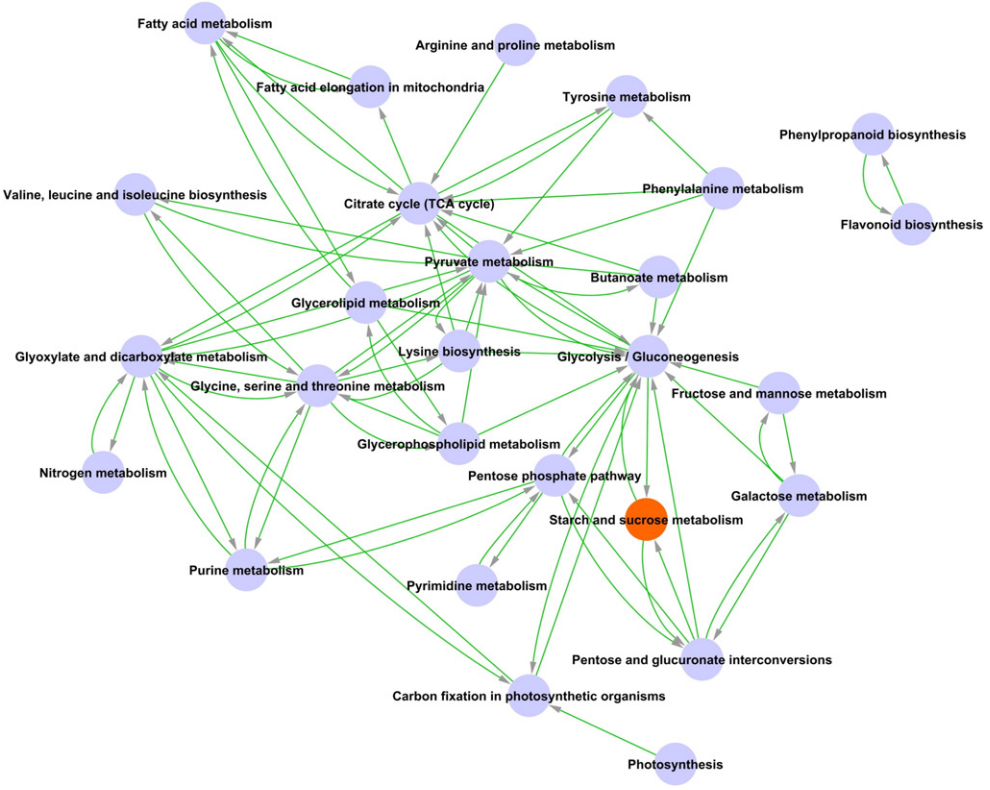

Fig. 7 – Metabolic pathway net established with significant pathways. Cycle nodes represent different pathways. Arrows represent the interaction between one pathway and another pathway by degree value. The source and points of arrows show the sources and targets of pathways in the network. More arrows at a node mean more pathways interacting with it, corresponding to greater importance of the pathway in the pathway net.

(55–75% of total dry grain weight), storage protein (10–15%), and lesser lipids. Thus, wheat grain development relies upon the synthesis and accumulation of starch and storage proteins. The activation and expression of stress-associated genes can protect plants from various biotic and abiotic stresses during grain development. Recently [21], transcriptome analysis during wheat grain development by RNA-Seq has been performed. It focused on cell type- and stage-dependent expression profiles and expression differences between different genomes. In this study, we used the GeneChip Wheat Genome Array for dynamic transcriptome profiling during grain development, focusing particularly on important differentially expressed genes involved in starch and protein synthesis and stress defense. The main metabolic pathways involved in wheat grain development are discussed in the following section.

4.1. *Activation of starch synthesis genes*

Carbohydrates are stored mainly in the form of starch in the wheat seed endosperm. Given that starch is the primary source of nutrition, seed germination requires adequate starch reserves. A previous study [20] using cDNA microarrays showed that the onset of wheat grain-filling occurred at 7–14 DPA, when genes encoding enzymes related to starch synthesis and storage protein synthesis were expressed at the highest levels. In the present study, we found that genes involved in sucrose and starch synthesis were activated at around 11 DPA, and that a large number of related genes were upregulated during starch accumulation (Fig. 5). Genes encoding enzymes involved in starch and storage proteins synthesis were expressed at their highest levels at 15–20 DPA.

The 14-3-3 proteins, a family of ubiquitous regulatory molecules that affect the activity of a broad range of targets by direct protein–protein interaction, are present in every eukaryotic organism and tissue [49,50]. This family regulates nitrogen and carbon assimilation, as well as various metabolic processes during plant development, including signal transduction, ATP production, peroxide detoxification, checkpoint control, apoptosis, and nutrient-sensing pathways [49,51]. In the present study, 14-3-3 proteins were revealed to be involved mainly in signaling-associated metabolic pathways, including signal reception, MAPK cascade reaction, and calcium regulation, with the cooperation of G proteins (Fig. S2). Previous research has shown that 14-3-3b transcript accumulation is inversely related to starch accumulation and may inhibit starch biosynthesis [20,51,52]. We found that the expression of the 14-3-3 gene was downregulated during grain-filling (Fig. 9, Fig. S2), indicating that 14-3-3 transcript accumulation and starch accumulation are negatively correlated, in agreement with the inhibition of starch biosynthesis by 14-3-3b transcript accumulation [20,51,52]. In contrast, G-protein genes were gradually upregulated during starch accumulation, especially at 15–20 DPA. This observation suggests that G-protein transcript accumulation and starch

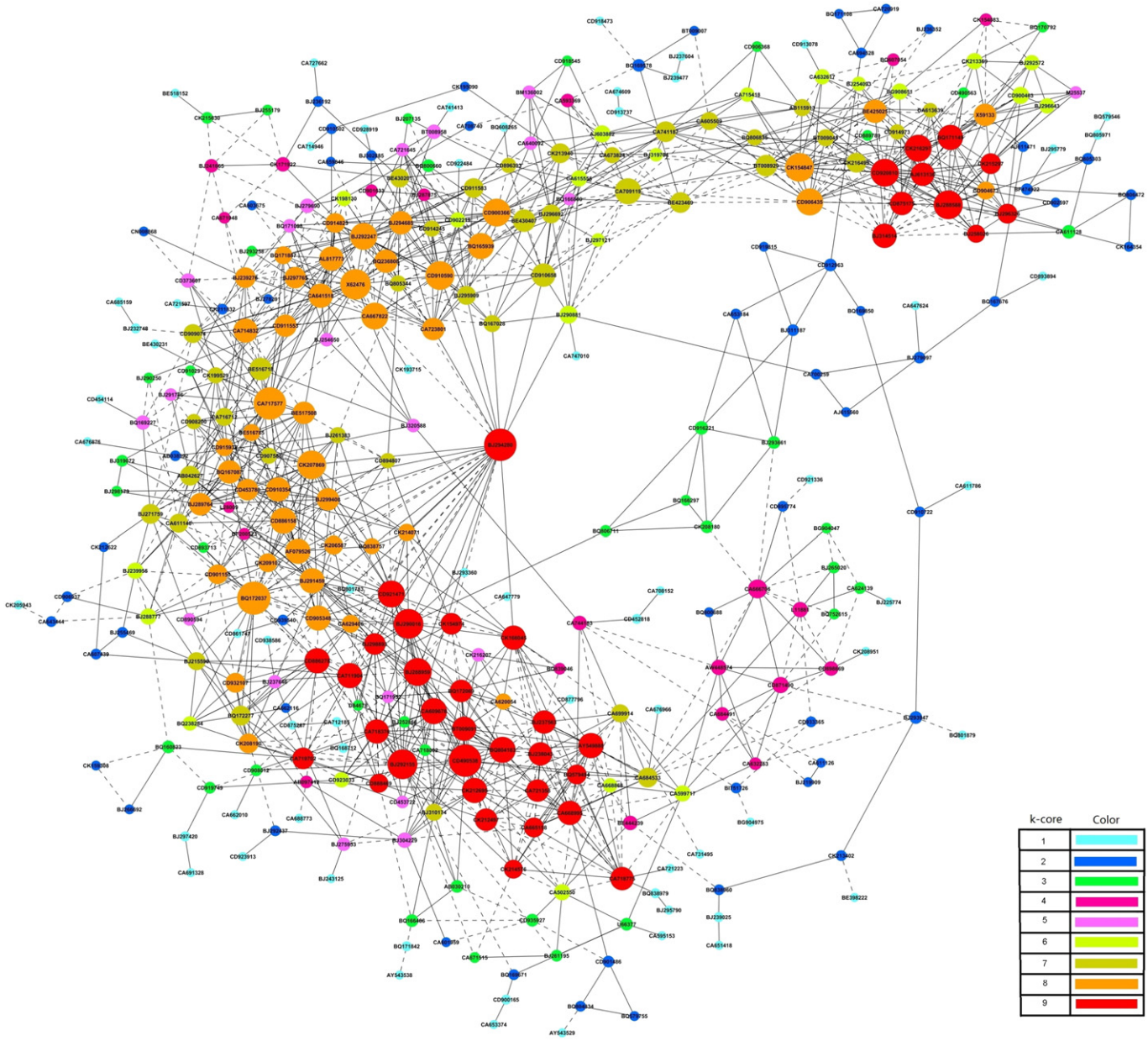

Fig. 8 – Gene co-expression network during seed development with k-core algorithm. Cycle nodes represent genes in the net. The sizes of nodes represent the strength of the interrelation among the nodes, and the edges between two nodes represent interactions between genes. The more edges on a gene, the more genes connect to it, and the more central the role it plays in the network. In the network, dashed lines represent negative and solid lines positive regulation.

accumulation are positively correlated, and that the upregulation of G protein genes could promote starch accumulation. Additionally, receptor kinase genes were largely upregulated from 11 to 20 DPA (Fig. 9, Fig. S2), suggesting that various signaling pathways are involved in starch gene activation and starch biosynthesis during grain development.

4.2. *Activation of protein synthesis genes*

Synthesis and accumulation are the major metabolic activities during the grain-filling period of seed development, and storage proteins are an important nutritive reserve during this stage. Prolamins, glutenins and gliadins are the main storage proteins and the major components of the gluten polymer [53]. The accumulation of these storage proteins affects wheat quality formation. All of the protein enzymes in wheat seed development are produced by the activation of protein synthesis genes.

Previous research has revealed that several enzymes involved in carbohydrate and protein metabolism (such as orthophosphate dikinase, aspartate aminotransferase, aspartic protease, and alanine aminotransferase) are most highly expressed at the transcript level at 14 DPA [54]. In the present study, we also identified several important enzyme families, such as cytochrome P450, peroxidases, UDP glycosyltransferases, O-methyltransferases, glutathione-S-transferases, and

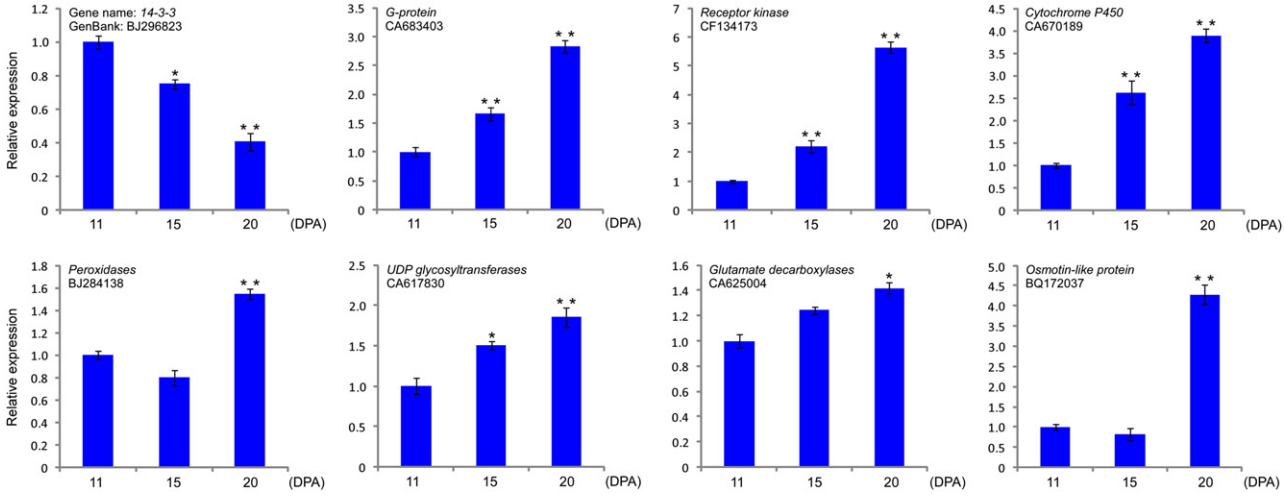

Fig. 9 – The dynamic expression patterns of eight important differentially expressed genes by qRT-PCR. The gene expression levels at 11 DPA were defined as 1.0. *P < 0.05, **P < 0.01.

beta-1,3-glucan hydrolases (Fig. S3). However, the expression of these enzymes tends be at its highest at around 20 DPA, several days later than the previously reported enzymes. Cytochrome P450 is a mixed-function oxidase with many important activities, including biosynthesis, detoxification, and stress resistance. Peroxidases play many roles in plant seeds, such as removing noxious H_2O_2, facilitating seed maturation by inhibiting IAA activity, and promoting ethylene synthesis. UDP glycosyltransferases are enzymes that can regulate the activity of donor molecules by transferring glycosyl from the activated donor molecule to the receptor. O-methyltransferases are responsible for amino transfer, which plays an important role in amino acid synthesis and protein synthesis. Glutathione-S-transferases are vital enzymes in seed development and have important detoxification functions. Beta-1,3-glucan hydrolases affect carbohydrate synthesis and degradation by hydrolyzing various glycosidic bonds. The appropriate activation and upregulation of all of these enzymes are critical for successful seed development.

4.3. *Activation of stress defense genes*

Seed development and maturation activate a series of mechanisms in response to various biotic and abiotic stresses, accompanied by an increased tolerance to desiccation [55]. In our results, genes involved in biotic and abiotic stresses were all upregulated during the accumulation of nutritive reserves (Fig. 6), particularly heat and drought/salt stress-associated genes. Drought, low temperatures, and salinity have dehydrating effects upon developmental stages, such as pollen and seeds [56,57], and late embryogenesis abundant (LEA) proteins are produced in response to such stimuli [58]. Interestingly, we found three important genes (CD913555, CD905348, and AY148491.1) encoding LEA proteins that belong to the functional group related to development (Table S1, Table S2). At the early grain-filling stage, upregulated genes comprised half of all the expressed genes in the group involved in development. After the grain-filling stages, most genes involved in development were upregulated gradually (Fig. 6). Thus, upregulation of development-related genes not only occurs in response to dehydrating stimuli, but also promotes the accumulation of storage reserves.

γ-Aminobutyric acid (GABA) is widely present in plants and plays important roles in plant growth and development. Studies on plants, such as *Arabidopsis* [59], rice [60] and sunflower [61], have shown that GABA has two highly important functions: the GABA shunt influences the TCA cycle and amino acid metabolism and GABA also provides protection from oxidative stress [60]. One previous study suggested that the accumulation of GABA in response to high temperatures corresponded to changes in glutamate decarboxylase and GABA transaminase activity [60]. Glutamate decarboxylase is synchronously upregulated with GABA and catalyzes GABA synthesis, while GABA transaminase induces GABA degradation. In the present study, we identified several genes encoding glutamate decarboxylase and GABA transaminase (Fig. 5, Table S1, Table S2). The genes encoding glutamate decarboxylase were marginally upregulated (Fig. 9), while GABA transaminase was downregulated. This finding suggests that GABA may be synthesized largely during the grain-filling stage and in response to oxidative stress. Low levels of O_2 have been found to induce GABA production by activating glutamate decarboxylase [62,63]. A similar result was reported in *Arabidopsis* mutants: GABA inhibited the accumulation of reactive oxygen species (ROS) [59]. This inhibition occurs likely because the GABA shunt can weaken the respiration of mitochondria in order to provide reaction substrates for the TCA cycle, such as NADH and succinate. In our results, photorespiration was repressed by the accumulation of GABA (Fig. 5): most genes involved in photorespiration were downregulated at 11–20 DPA.

Acknowledgments

This research was financially supported by grants from the National Natural Science Foundation of China (31471485),

Natural Science Foundation of Beijing City and the Key Developmental Project of Science and Technology from Beijing Municipal Commission of Education (KZ201410028031).

Supplementary material

Supplementary data for this article can be found online at http://dx.doi.org/10.1016/j.cj.2016.01.006.

REFERENCES

[1] P.R. Shewry, Wheat, J. Exp. Bot. 60 (2009) 1537–1553.
[2] Y.L. Yu, G.F. Guo, D.W. Lv, Y.K. Hu, J.R. Li, X.H. Li, Y.M. Yan, Transcriptome analysis during seed germination of elite Chinese bread wheat cultivar Jimai 20, BMC Plant Biol. 14 (2014) 20, http://dx.doi.org/10.1186/1471-2229-14-20.
[3] P. Aquino, F. Carron, R. Calvo, Selected wheat statistics, in: P.L. Pingali (Ed.), CIMMYT 1998–1999 World Wheat Facts and Trends, Global Wheat Research in a Changing World: Challenges and Achievements, CIMMYT, D.F. Mexico 1999, pp. 33–45.
[4] E. Triboi, A.M. Triboi-Blondel, Productivity and grain orseed composition: a new approach to an old problem–invited paper, Eur. J. Agron. 16 (2002) 163–186.
[5] A. Jerkovic, A.M. Kriegel, J.R. Bradner, B.J. Atwell, T.H. Roberts, R.D. Willows, Strategic distribution of protective proteins within bran layers of wheat protects the nutrient-rich endosperm, Plant Physiol. 152 (2010) 1459–1470.
[6] S.A. Gillies, A. Futardo, R.J. Henry, Gene expression in the developing aleuroneand starchyendosperm of wheat, Plant Biotechnol. J. 10 (2012) 668–679.
[7] D. Simmonds, T. O'Brien, Morphological and biochemical development of the wheat endosperm, Adv. Cereal Sci. Technol. 4 (1981) 5–70.
[8] A.A. Khan, The physiology and biochemistry of seed development, dormancy and germination, in: A.A. Khan (Ed.), The Physiology and Biochemistry of Seed Development, Dormancy and Germination, Elsevier Biomedical, Amsterdam, Netherlands, 1982.
[9] C. Finnie, S. Melchior, P. Roepstorff, B. Svensson, Proteome analysis of grain filling and seed maturation in barley, Plant Physiol. 129 (2002) 1308–1319.
[10] J.S. Shi, Y. Zhen, R.H. Zheng, Proteome profiling of early seed development in *Cunninghamia lanceolata* (Lamb.) Hook, J. Exp. Bot. 61 (2010) 2367–2381.
[11] K. Gallardo, C.L. Signor, J. Vandekerckhove, R.D. Thompson, J. Burstin, Proteomics of *Medicago truncatula* seed development establishes the time frame of diverse metabolic processes related to reserve accumulation, Plant Physiol. 133 (2003) 664–682.
[12] J.S. Greenwood, J.D. Bewley, Seed development in *Ricinus communis* (Castor Bean): I. Descriptive morphology, Can. J. Bot. 60 (2011) 1751–1760.
[13] S. Dam, B.S. Laursen, J.H. Ørnfelt, B. Jochimsen, H.H. Stærfeldt, C. Friis, K. Nielsen, N. Goffard, S. Besenbacher, L. Krusell, S. Sato, S. Tabata, I.B. Thøgersen, J.J. Enghild, J. Stougaard, The proteome of seed development in the model legumelotus japonicas, Plant Physiol. 149 (2009) 1325–1340.
[14] G.F. Guo, D.W. Lv, X. Yan, S. Subburaj, P. Ge, X.H. Li, Y.K. Hu, Y.M. Yan, Proteome characterization of developing grains in bread wheat cultivars (*Triticum aestivum* L.), BMC Plant Biol. 12 (2012) 147, http://dx.doi.org/10.1186/1471–2229-12-147.
[15] L. Dure, L. Waters, Long-lived messenger RNA: evidence from cotton seed germination, Science 147 (1965) 410–412.
[16] C. Almoguera, J. Jordano, Development and environment concurrent expression of sunflower dry-seed-stored low-molecular-weight heat-shock protein and Lea mRNAs, Plant Mol. Biol. 19 (1992) 781–792.
[17] N. Ishibashi, D. Yamauchi, T. Minamikawa, Stored mRNA in cotyledons of *Vigna unguiculata* seeds: nucleotide sequence of cloned cDNA for a stored mRNA and induction of its synthesis by precocious germination, Plant Mol. Biol. 15 (1990) 59–64.
[18] J. Kuligowski, M. Ferrand, E. Chenou, Stored mRNA in early embryos of a fern marsileavestita: a paternal and maternal origin, Mol. Reprod. Dev. 30 (1991) 27–33.
[19] Y.F. Wan, R.L. Poole, A.K. Huttly, C. Toscano-Underwood, K. Feeney, S. Welham, M.J. Gooding, C. Mills, K.J. Edwards, P.R. Shewry, R.A.C. Mitchell, Transcriptome analysis of grain development in hexaploid wheat, BMC Genomics 9 (2008) 121, http://dx.doi.org/10.1186/1471-2164-9-121.
[20] D.L. Laudencia-Chingcuanco, B.S. Stamova, F.M. You, G.R. Lazo, D.M. Beckles, O.D. Anderson, Transcriptional profiling of wheat caryopsis development using cDNA microarrays, Plant Mol. Biol. 63 (2007) 651–668.
[21] M. Pfeifer, K.G. Kugler, S.R. Sandve, B.J. Zhan, H. Rudi, T.R. Hvidsten, International wheat genome sequencing consortium, in: K.F.X. Mayer, O.A. Olsen (Eds.),Genome Interplay in the Grain Transcriptome of Hexaploid Bread Wheat, Science, 345 2014, p. 1250091, http://dx.doi.org/10.1126/science.1250091.
[22] R. Brenchley, M. Spannagl, M. Pfeifer, G.L.A. Barker, R. D'Amore, A.M. Allen, N. McKenzie, M. Kramer, A. Kerhornou, D. Bolser, S. Kay, D. Waite, M. Trick, I. Bancroft, Y. Gu, N. Huo, M.C. Luo, S. Sehgal, B. Gill, S. Kianian, O. Anderson, P. Kersey, J. Dvorak, W.R. McCombie, A. Hall, K.F.X. Mayer, K.J. Edwards, M.W. Bevan, N. Hall, Analysis of the bread wheat genome using whole-genome shotgun sequencing, Nature 491 (2012) 705–710.
[23] H.Q. Ling, J. Wang, S.C. Zhao, D.C. Liu, J.Y. Wang, H. Sun, C. Zhang, H.J. Fan, D. Li, L.L. Dong, Y. Tao, C. Gao, H.L. Wu, Y.W. Li, Y. Cui, X.S. Guo, S.S. Zheng, B. Wang, K. Yu, Q.S. Liang, W.L. Yang, X.Y. Lou, J. Chen, M.J. Feng, J.B. Jian, X.F. Zhang, G.B. Luo, Y. Jiang, J.J. Liu, Z.B. Wang, Y.H. Sha, B.R. Zhang, H.J. Wu, D.Z. Tang, Q.H. Shen, P.Y. Xue, S.H. Zou, X.J. Wang, X. Liu, F.M. Wang, Y.P. Yang, X.L. An, Z.Y. Dong, K.P. Zhang, X.Q. Zhang, M.C. Luo, J. Dvorak, Y.P. Tong, J. Wang, H.M. Yang, Z.S. Li, D.W. Wang, A.M. Zhang, Draft genome of the wheat A-genome progenitor *Triticum urartu*, Nature 496 (2013) 87–90.
[24] J.Z. Jia, S.C. Zhao, X.Y. Kong, Y.R. Li, G.Y. Zhao, W.M. He, R. Appels, M. Pfeifer, Y. Tao, X.Y. Zhang, R.L. Jing, C. Zhang, Y.Z. Ma, L.F. Gao, C. Gao, M. Spannagl, K.F.X. Mayer, D. Li, S.K. Pan, F.Y. Zheng, Q. Hu, X.C. Xia, J.W. Li, Q.S. Liang, J. Chen, T. Wicker, C.Y. Gou, H.H. Kuang, G.Y. He, Y.D. Luo, B. Keller, Q.J. Xia, P. Lu, J.Y. Wang, H.F. Zou, R.Z. Zhang, J.Y. Xu, J.L. Gao, C. Middleton, Z.W. Quan, G.M. Liu, J. Wang, H.M. Yang, X. Liu, Z.H. He, L. Mao, J. Wang, *Aegilops tauschii* draft genome sequence reveals a gene repertoire for wheat adaptation, Nature 496 (2013) 91–95.
[25] J.C. Luo, J.G. Jiao, D.C. Ren, J.J. Liu, The new wheat cultivar Jimai 20 with high yield and good quality, J. Triticeae Crops 26 (1) (2006) 159 (in Chinese).
[26] G.W. Wright, R.M. Simon, A random variance model for detection of differential gene expression in small microarray experiments, Bioinformatics 19 (2003) 2448–2455.
[27] H.Y. Yang, N. Crawford, L. Lukes, R. Finney, M. Lancaster, K.W. Hunter, Metastasis predictive signature profiles pre-exist in normal tissues, Clin. Exp. Metastas 22 (2005) 593–603.
[28] R. Clarke, H.W. Ressom, A. Wang, J. Xuan, M.C. Liu, E.A. Gehan, Y. Wang, The properties of high-dimensional data spaces: implications for exploring gene and protein expression data, Nat. Rev. Cancer 8 (2008) 37–49.

[29] M.F. Ramoni, P. Sebastiani, S. KohaneI, Cluster analysis of gene expression dynamics, Proc. Natl. Acad. Sci. U. S. A. 99 (2002) 9121–9126.
[30] L.D. Miller, P.M. Long, L. Wong, S. Mukherjee, L.M. McShane, E.T. Liu, Optimal gene expression analysis by microarrays, Cancer Cell 2 (2002) 353–361.
[31] H.B. Dong, S.Q. Wang, Y.Y. Jia, Y.D. Ni, Y.S. Zhang, S. Zhuang, X.Z. Shen, R.Q. Zhao, Long-term effects of subacute ruminal acidosis (SARA) on milk quality and hepatic gene expression in lactating goats fed a high-concentrate diet, PLoS One 8 (2013), e82850, http://dx.doi.org/10.1371/journal.pone.0082850.
[32] Gene Ontology Consortium, The Gene Ontology (GO) project in 2006, Nucleic Acids Res. 34 (2006) D322–D326.
[33] The Gene Ontology Consortium, M. Ashburner, C.A. Ball, J.A. Blake, D. Botstein, H. Butler, J.M. Cherry, A.P. Davis, K. Dolinski, S.S. Dwight, J.T. Eppig, M.A. Harris, D.P. Hill, L. Issel-Tarver, A. Kasarskis, S. Lewis, J.C. Matese, J.E. Richardson, M. Ringwald, G.M. Rubin, G. Sherlock, Gene ontology: tool for the unification of biology, Nat. Genet. 25 (2000) 25–29.
[34] B. Usadel, A. Nagel, O. Thimm, H. Redestig, O.E. Blaesing, N. Palacios-Rojas, J. Selbig, J. Hannemann, M.C. Piques, D. Steinhauser, W.R. Scheible, Y. Gibon, R. Morcuende, D. Weicht, S. Meyer, M. Stitt, Extension of the visualization tool MapMan to allow statistical analysis of arrays, display of corresponding genes, and comparison with known responses, Plant Physiol. 138 (2005) 1195–1204.
[35] K. Nakabayashi, M. Okamoto, T. Koshiba, Y. Kamiya, E. Nambara, Genome-wide profiling of stored mRNA in *Arabidopsis thaliana* seed germination: epigenetic and genetic regulation of transcription in seed, Plant J. 41 (2005) 697–709.
[36] M. Kanehisa, S. Goto, S. Kawashima, Y. Okuno, M. Hattori, The KEGG resource for deciphering the genome, Nucleic Acids Res. 32 (2004) D277–D280.
[37] M. Yi, J.D. Horton, J.C. Cohen, H.H. Hobbs, R.M. Stephens, Whole pathway scope: a comprehensive pathway-based analysis tool for high-throughput data, BMC Bioinformatics 7 (2006) 30, http://dx.doi.org/10.1186/1471-2105-7-30.
[38] S. Draghici, P. Khatri, A.L. Tarca, K. Amin, A. Done, C. Voichita, C. Georgescu, R. Romero, A systems biology approach for pathway level analysis, Genome Res. 17 (2007) 1537–1545.
[39] V. Vermeirssen, M.I. Barrasa, C.A. Hidalgo, J.A.B. Babon, R. Sequerra, L. Doucette-Stamm, A.L. Barabási, A.J.M. Walhout, Transcription factor modularity in a gene-centered *C. elegans* core neuronal protein-DNA interaction network, Genome Res. 17 (2007) 1061–1071.
[40] W. Huber, V.J. Carey, L. Long, S. Falcon, R. Gentleman, Graphs in molecular biology, BMC Bioinf. 8 (Suppl. 6) (2007) S8, http://dx.doi.org/10.1186/1471–2105-8-S6-S8.
[41] E. Ravasz, A.L. Somera, D.A. Mongru, Z.N. Oltvai, A.L. Barabási, Hierarchical organization of modularity in metabolic networks, Science 297 (2002) 1551.
[42] A.L. Barabási, Z.N. Oltvai, Network biology: understanding the cell's functional organization, Nat. Rev. Genet. 5 (2004) 101–113.
[43] K.J. Livak, T.D. Schmittgen, Analysis of relative gene expression data using real-time quantitative PCR and the $2^{-\Delta\Delta CT}$ method, Methods 25 (2001) 402–408.
[44] D.B. Bechtel, J.D. Wilson, Amyloplast formation and starch granule development in hard red winter wheat, Cereal Chem. 80 (2003) 175–183.
[45] J.D. Wilson, D.B. Bechtel, T.C. Todd, P.A. Seib, Measurement of wheat starch granule size distribution using image analysis and laser diffraction technology, Cereal Chem. 83 (2006) 259–268.
[46] A.R. Fernie, F. Carrari, L.J. Sweetlove, Respiratory metabolism: glycolysis, the TCA cycle and mitochondrial electron transport, Curr. Opin. Plant Biol. 7 (2004) 254–261.
[47] K. Eimerta, P. Villanda, A. Kilianc, L.A. Kleczkowski, Cloning and characterization of several cDNAs for UDP-glucose pyrophosphorylase from barley (*Hordeum vulgare*) tissues, Gene 170 (1996) 227–232.
[48] T. Rees, M. Leja, F.D. Macdonald, J.H. Green, Nucleotide sugars and starch synthesis in spadix of *Arum maculatum* and suspension cultures of *Glycine max*, Phytochemistry 23 (1984) 2463–2468.
[49] H. Fulgosi, J. Soll, F.S. Maraschin, H.A.A.J. Korthout, M. Wang, C. Testerink, 14-3-3 proteins and plant development, Plant Mol. Biol. 50 (2002) 1019–1029.
[50] M. Lancien, T.C. McCabe, C. Chang, M.R. Roberts, Roles for plant 14-3-3 proteins in signaling and development, Comp. Biochem. Physiol. Part A 141 (2005) S258–S259.
[51] R.J. Ferl, 14-3-3 proteins and signal transduction, Annu. Rev. Plant Physiol. Plant Mol. Biol. 47 (1996) 49–73.
[52] P.C. Sehnke, H.J. Chung, K. Wu, R.J. Ferl, Regulation of starch accumulation by granule associated plant 14-3-3 proteins, Proc. Natl. Acad. Sci. U. S. A. 98 (2001) 765–770.
[53] P.R. Shewry, N.G. Halford, Cereal seed storage proteins: structures, properties and role in grain utilization, J. Exp. Bot. 53 (2002) 947–958.
[54] I.J. Tetlow, M.K. Morell, M.J. Emes, Recent developments in understanding the regulation of starch metabolism in higher plants, J. Exp. Bot. 55 (2004) 2131–2145.
[55] C. Finnie, S. Melchior, P. Roepstorff, B. Svensson, Proteome analysis of grain filling and seed maturation in barley, Plant Physiol. 129 (2002) 1308–1319.
[56] J. Danyluk, A. Perron, M. Houde, A. Limin, B. Fowler, N. Benhamou, F. Sarhan, Accumulation of an acidic dehydrin in the vicinity of the plasma membrane during cold acclimation of wheat, Plant Cell 10 (1998) 623–638.
[57] S.A. Campbell, T.J. Close, Dehydrins: genes, proteins, and associations with phenotypic traits, New Phytol. 137 (1997) 61–74.
[58] J.M. Farrant, C. Bailly, J. Leymarie, B. Hamman, D. Come, F. Corbineau, Wheat seedlings as a model to understand desiccation tolerance and sensitivity, Plant Physiol. 120 (2004) 563–574.
[59] A. Fait, A. Yellin, H. Fromm, GABA shunt deficiencies and accumulation of reactive oxygen intermediate, insight from *Arabidopsis* mutants, FEBS Lett. 579 (2005) 415–420.
[60] H. Yamakawa, M. Hakata, Atlas of rice grain filling-related metabolism under high temperature: joint analysis of metabolome and transcriptome demonstrated inhibition of starch accumulation and induction of amino acid accumulation, Plant Cell Physiol. 51 (2010) 795–809.
[61] H. Rolletschek, L. Borisjuk, A. Sánchez-García, C. Gotor, L.C. Romero, J.M. Martínez-Rivas, M. Mancha, Temperature-dependent endogenous oxygen concentration regulates microsomal oleatedesaturase in developing sunflower seeds, J. Exp. Bot. 58 (2007) 3171–3181.
[62] N. Aurisano, A. Bertani, R. Reggiani, Involvement of calciumand calmodulin in protein and amino acid metabolism in rice rootsunder anoxia, Plant Cell Physiol. 36 (1995) 1525–1529.
[63] R. Reggiani, C.A. Cantu, I. Brambilla, A. Bertani, Accumulation and interconversion of amino acids in rice rootsunder anoxia, Plant Cell Physiol. 29 (1988) 981–987.